Probing the structures of gas-phase rhodium cluster cations by far-infrared spectroscopy

D. J. Harding,[1,2] P. Gruene,[1] M. Haertelt,[1] G. Meijer,[1] A. Fielicke,[1,a] S. M. Hamilton,[3] W. S. Hopkins,[3] S. R. Mackenzie,[3] S. P. Neville,[2] and T. R. Walsh[2,4,b]

[1]*Fritz-Haber-Institut der Max-Planck-Gesellschaft, Faradayweg 4-6, D-14195 Berlin, Germany*
[2]*Department of Chemistry, University of Warwick, Coventry CV4 7AL, United Kingdom*
[3]*Department of Chemistry, Physical and Theoretical Chemistry Laboratory, University of Oxford, South Parks Road, Oxford OX1 3QZ, United Kingdom*
[4]*Centre for Scientific Computing, University of Warwick, Coventry CV4 7AL, United Kingdom*

The geometric structures of small cationic rhodium clusters Rh_n^+ ($n = 6$–12) are investigated by comparison of experimental far-infrared multiple photon dissociation spectra with spectra calculated using density functional theory. The clusters are found to favor structures based on octahedral and tetrahedral motifs for most of the sizes considered, in contrast to previous theoretical predictions that rhodium clusters should favor cubic motifs. Our findings highlight the need for further development of theoretical and computational methods to treat these high-spin transition metal clusters. © *2010 American Institute of Physics*. [doi:10.1063/1.3509778]

I. INTRODUCTION

The ability to make an unambiguous assignment of the geometric structures of transition-metal (TM) clusters would represent a significant step toward a deeper understanding of the remarkable size- and structure-dependent properties of TM clusters.[1,2] These properties are of interest for fundamental reasons to observe their evolution from the atom and dimer toward the bulk.[3] TM clusters also serve as model systems for heterogeneous catalysis[1] where, in many cases, finely divided metal particles form the active sites.

Rhodium clusters have been the subject of a number of experimental studies due to interest in the catalytic properties of the metal. The magnetic moments,[4,5] electric polarizability,[6] and reactivity with a range of small molecules[7–16] have been investigated, in many instances revealing a significant size dependence of these properties. In several cases, reaction rate measurements on monodisperse cluster samples have suggested multiple reactivities, indicating the presence of multiple forms of clusters of the same size.[12,13,16] This behavior has previously been ascribed to the coexistence of different geometric isomers in these systems.[10]

Electronic structure calculations on late TM clusters remain challenging, principally due to a combination of three factors: the large number of electrons, the large number of possible geometric isomers, and the range of spin multiplicities that must be considered. For rhodium and other late TM clusters, a wide range of geometric motifs have been suggested as low-energy structures, primarily on the basis of density functional theory (DFT) calculations. These structures generally fall into one of two categories: those based on close-packed octahedral and polytetrahedral units,[17–20] and those with more open motifs based on square and cubic units.[21–24] Comparison of the performance of different functionals when applied to small, late TM clusters[25–27] indicates that the favored class of structural motif (either close-packed or open) is dependent on whether the functional under consideration is purely density dependent or a hybrid, including a portion of Hartree–Fock (exact) exchange. While these data demonstrate the sensitivity of the theoretical results to the details of the calculations, they provide little guidance as to the real structures of the clusters. Contemporary exchange-correlation functionals have typically been developed either for small molecules or for bulk systems and tested against datasets that do not contain information on late TM clusters. We cannot, therefore, expect that these functionals will perform reliably for these clusters. However, the issues with electronic structure theory relate to only one aspect of this study; that of creating a faithful representation of the potential energy landscape (PEL) for TM clusters. The other significant challenge in this endeavor is ensuring a thorough exploration of this PEL, and connecting the resulting PEL structure with the dynamical and equilibrium properties of the clusters.[28] Given these challenges, the partnership of experiment with theory provides a powerful means to test the quality of the theoretical treatment of these nonstandard systems. Alongside much-needed developments in multireference calculations for late TM clusters of the sizes considered here, significant advances can be made in realizing the goal of linking cluster properties with known structural details.

Spectroscopic investigations of rhodium clusters, which can provide experimental details of their structure, are limited. The stretching frequency[29] and bond dissociation energy[30] of the dimer have been measured, while electron spin resonance spectroscopy determined the trimer to have D_{3h} symmetry.[31] We have recently reported a combined far-infrared multiple photon dissociation (FIR-MPD) spectroscopy and DFT study of Rh_8^+, from which we determined the structure to be a bicapped octahedron (bc-oh).[32] This study was a significant advance, since previous calculations (in the absence of

[a]Author to whom correspondence should be addressed. Electronic mail: fielicke@fhi-berlin.mpg.de.
[b]Author to whom correspondence should be addressed. Electronic mail: t.walsh@warwick.ac.uk.

experimental data) had suggested that the cube structure was the global minimum. The use of hybrid exchange-correlation functionals was pivotal to the success of our previous study. Here, we build further on this study and report the results for the clusters Rh_n^+, $n = 6$–12.

II. COMPUTATIONAL METHODS

Given the variety of structural motifs predicted in the literature for rhodium and other late TM clusters, a thorough search of the cluster PEL is important. We used a two-step process to determine the low-energy structures of the clusters. In the first step, we used basin-hopping (BH) Monte Carlo (MC) simulation[33] to explore the PEL of the clusters and identify candidate structures. In these BH simulations, we generate the PEL "on the fly" with a local optimization and energy evaluation at each MC step, and are free, in principle, to use any method to describe the PEL. In order to maximize the chances of finding the important, low-energy structures of the clusters we have used two different approaches to represent the PEL. In one set of runs we used DFT; in a completely different set of runs we used the Sutton–Chen model potential.[34] Because these two approaches favor markedly different motifs for rhodium clusters, we expected this procedure would yield a suitable range of candidate structures. Both sets of BH runs followed the procedure as outlined previously.[35] For the DFT-BH runs, our BH code was interfaced with the GAUSSIAN 03 program[36] which performed the DFT energy evaluation and local optimization at the SVWN/LANL2MB level of theory.[37,38] In the second step, the candidate structures resulting from our BH simulations were reoptimized without symmetry constraints in a range of spin multiplicities using the PBE (Ref. 39) generalized gradient approximation (GGA) and PBE1 (Ref. 40) hybrid-GGA functionals with the Stuttgart/Dresden SDD (Ref. 41) effective core potential (ECP) and basis set for Rh_6^+ and the LANL2DZ (Ref. 42) ECP and basis set for the larger clusters. The range of spin multiplicities varied for each cluster geometry; we essentially explored all relevant multiplicities for a given structure such that we had identified the optimum spin multiplicity for that geometry. The GAUSSIAN 03 package[36] was used for these DFT calculations. The argon messenger atom(s) were not explicitly included in the calculations as the experimental spectra were essentially unchanged for clusters with different numbers of messenger atoms.

The vibrational spectra were calculated from analytic second derivatives. For ease of comparison with the experimental spectra, the resulting stick spectra were broadened with a Gaussian line shape function of 6 cm^{-1} full width at half maximum height. The frequencies calculated at the PBE1 level are shown without scaling. In the following comparisons of experiment and theory we have highlighted in red the spectra of the isomers that we suggest provide the best match. Following comparison across the different sizes, a scaling factor slightly less than 1 (0.96–0.98) might improve the agreement slightly. The relative energies are reported without corrections for the zero-point vibrational energy (ZPVE) as the differences in ZPVE between the different isomers were found to be small. For Rh_9^+, we calculated the relative abun-

dance of a range of isomers using the harmonic superposition approximation[43] (HSA) in the microcanonical ensemble, as described previously.[44,45] We have also performed calculations at the hybrid-meta-GGA TPSSh/def2-TZVP level using Turbomole.[46–50] The hybrid form TPSSh was chosen because of the high performance of the pure density dependent form TPSS for calculations on gold[51] and tantalum[52] clusters and our observation of the importance, for rhodium clusters, of including a portion of partial exact exchange.[32]

III. FIR-MPD SPECTROSCOPY

The experiment and data analysis procedure have been described in detail previously.[53,54] In order to measure vibrational spectra of bare TM clusters we use the messenger-atom technique with argon as the messenger. Argon-tagged clusters are generated by pulsed laser ablation (532 nm, ca. 10 mJ per pulse) of a rotating rhodium rod, the resulting plasma is quenched and carried along a cooled channel (173 K) by a mixture of argon (0.3%) in helium before expansion into vacuum and passage through a skimmer. The resulting cluster beam passes through an aperture and into the extraction region of a reflectron time of flight mass spectrometer. The infrared (IR) beam from the Free Electron Laser for Infrared eXperiments (FELIX) (Ref. 55) counterpropagates along the molecular beam axis. Vibrational spectra are obtained by monitoring the depletion of the argon-tagged complexes as a function of FELIX wavelength. Long-term drift in the cluster signal is accounted for by measuring reference spectra without FELIX radiation on alternate shots.

The maximum level of depletion which could be achieved for the argon-tagged rhodium clusters was rather low, about 50%. This may be due to intrinsically small IR cross sections of the complexes or to relatively strong binding of the argon atoms to the rhodium clusters. We note that in cases where only low levels of depletion were observed it has not been possible to rule out the presence of multiple isomers.

IV. RESULTS

Using both the PBE and PBE1 functionals the clusters were found to favor high-spin multiplicities, consistent with the large magnetic moments measured for neutral rhodium clusters.[5] PBE1 favored slightly higher multiplicities than PBE, presumably due to Hartree–Fock's favoring of open-shell systems.[56] As we have previously reported,[32] the choice of the PBE or PBE1 functionals changed the favored geometry of the Rh_8^+ cluster from cubic to a close-packed bicapped octahedron (bc-oh), presumably due to the inclusion of a portion of partial exact exchange in PBE1. We have found similar effects for most cluster sizes in the range ($n = 6$–12) that we discuss here, where it was seen that geometries with square or cubic motifs were favored by PBE whilst close-packed geometries were favored by PBE1. Given the much better agreement obtained with the PBE1 calculations[32] we will only show these results here, with the results of the PBE calculations presented in the electronic supplementary information (ESI).[57] The results of our calculations at the TPSSh/def2-TZVP level were generally similar to those at the PBE1 level.
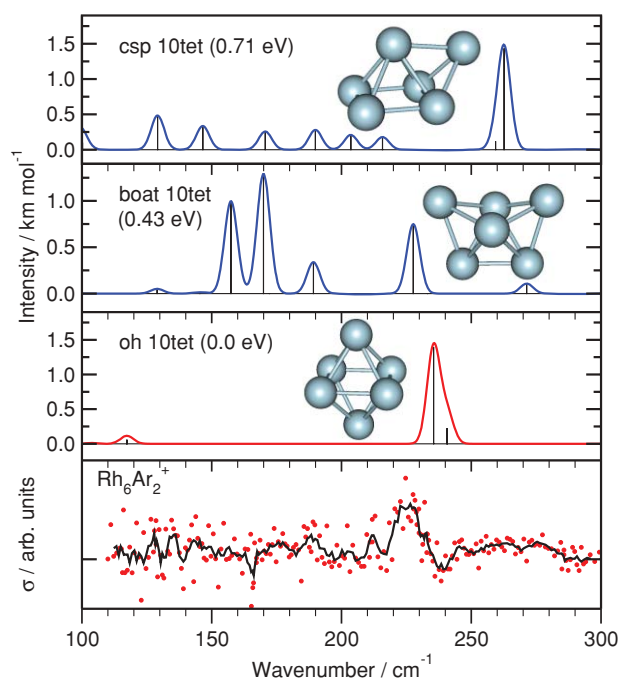
FIG. 1. Comparison of experimental FIR-MPD spectrum of $Rh_6Ar_2^+$ and spectra calculated at the PBE1/SDD level of theory. The experimental cross section σ is in arbitrary units, the experimental data is shown by the dots and the black line is a three-point running average to the data. The calculated intensities are in km mol^{-1}.

Over the size range we have investigated, only a few cases showed significantly better agreement between experimental and calculated spectra, while in some cases, notably Rh_8^+, the agreement was significantly worse. The results are shown in the ESI.

A. Rh_6^+

The experimental FIR-MPD spectra obtained for $Rh_6Ar_{1,2}^+$ clusters show particularly low levels of depletion, probably due to intrinsically small IR cross sections (*vide infra*), resulting in a rather noisy spectrum.

Rh_6^+ is one of the two sizes where both pure- and hybrid-DFT favored the same geometric isomer, with both predicting distorted octahedral (oh) structures. The ordering of the higher energy isomers was, however, different. The trigonal prism, which was the second lowest energy isomer at the PBE/SDD level,[35] was found to be a saddle point at the PBE1/SDD level. Figure 1 shows the comparison of the experimental FIR-MPD spectrum of $Rh_6Ar_2^+$ and calculated spectra at the PBE1/SDD level. The agreement between the experimental spectrum and the calculated spectrum of the lowest energy distorted octahedron isomer (actually a slightly distorted square bipyramid) in a 10tet electronic state is relatively good, both having essentially a single, rather broad feature, at *ca.* 225 cm^{-1} for the experiment and 235 cm^{-1} for the calculation. The other two low-energy isomers (a capped square pyramid (csp) and the boat structure) both have calculated spectra which fit the experimental spectrum less well. The calculated IR cross sections of all three isomers are low (ca. 1.5 km mol^{-1}) compared to those of many of the larger clusters (ca. 4 km mol^{-1}).

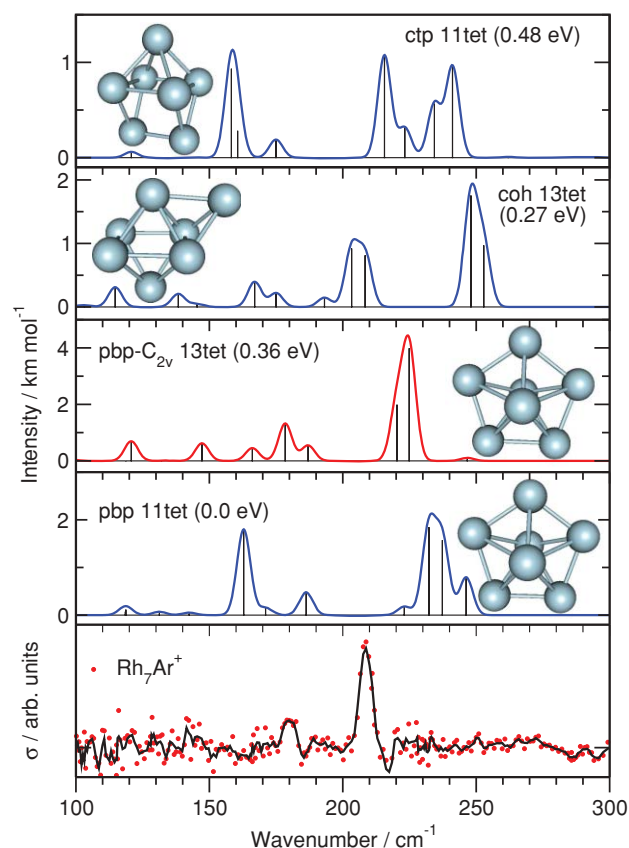FIG. 2. FIR-MPD spectrum of Rh_7Ar^+ and calculated spectra of Rh_7^+ at the PBE1/LANL2DZ level.

Rh_6^+ is one of a number of sizes for which there is evidence of multiple forms of the cluster with different reactivities.[12,16] Here, however, while we see no evidence of a second isomer, the low level of depletion prevents us from excluding this possibility.

B. Rh_7^+

Rh_7^+ is the other size for which we found both PBE and PBE1 to favor the same isomer, a (distorted) pentagonal bipyramid (pbp). At the PBE1/LANL2DZ level, two different forms of the pbp, belonging to point groups C_1 and C_{2v}, of 11tet spin multiplicity were the lowest energy structures we found. The interatomic distances around the five-atom ring vary by ~ 0.05 Å in both cases. As their calculated spectra are almost identical we show only one in Fig. 2, although this does not provide a particularly good match to the experimental spectrum. While there are two main features, the spacing between them is significantly larger in the calculated spectrum than in the experiment (60 cm^{-1} cf. 30 cm^{-1}). A 13tet C_{2v} pbp isomer provides a somewhat better match to the experimental spectrum, matching the position of the low-frequency band to within 5 cm^{-1}, the high-frequency band to *ca.* 15 cm^{-1} and their relative intensities. However, this structure is 0.36 eV higher in energy than the 11tet putative global minimum. The splitting between the different modes was found to be very sensitive to fine details of the structure and the spin multiplicity, and in the C_1 13tet (not shown) the modes split
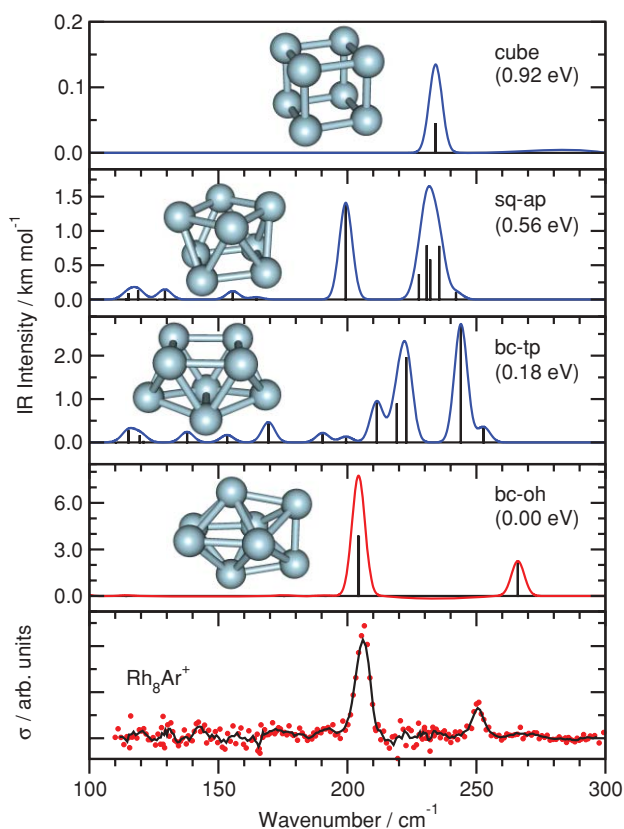
FIG. 3. FIR-MPD spectrum of Rh_8Ar^+ and calculated spectra of Rh_8^+ at the PBE1/LANL2DZ level.

FIG. 4. FIR-MPD spectrum of Rh_9Ar^+ and calculated spectra of Rh_9^+ at the PBE1/LANL2DZ level.

further, giving six distinct features after the Gaussian broadening. The poor match provided by the other low-energy isomers supports our assignment of a distorted pbp structure for Rh_7^+.

There are a number of reasons why the agreement between experiment and theory might be so poor in this case, and we speculate that dynamic processes (e.g., a pseudorotation moving the long bond around the five-atom ring) or static electronic correlation may be particularly important for the pbp isomer. Another possibility is simply that we have not found the precise slightly distorted pbp structure of lowest energy.

Beyer and Knickelbein[6] have reported that neutral Rh_7 has a permanent dipole moment, which would preclude a perfect D_{5h} pbp structure. These authors instead suggested a C_{3v} capped octahedron (coh) as a possible alternative structure. However, the spectra we calculated for such coh isomers were a poor match with experiment. Such a comparison between charged and neutral systems should clearly be treated with care. In particular, it is possible that different isomers are favored by the different charge states, as is the case for gold clusters.[51,58,59]

C. Rh_8^+

The details of the results for Rh_8^+ have been reported previously.[32] For completeness, here we show the experimental spectrum and the calculated spectra at the PBE1/LANL2DZ level (see Fig. 3). At this level, the lowest
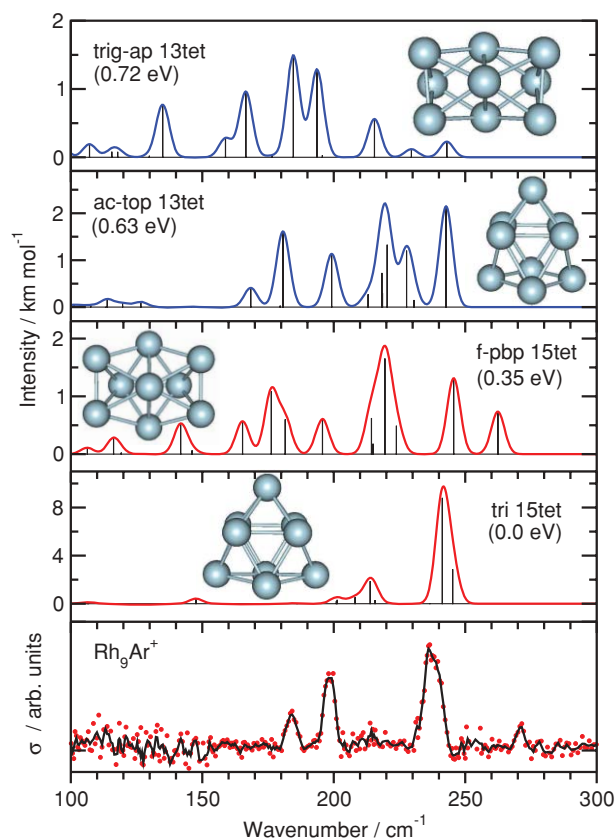
energy structure we found was a bicapped octahedron isomer (bc-oh) in a 12tet spin multiplicity, the calculated spectrum provides a relatively good match to the experimental spectrum though the small feature at 266 cm^{-1} is blue shifted by 15 cm^{-1} compared to experiment. The calculated spectra of the other, higher energy, isomers all fit the experimental spectrum less well.

D. Rh_9^+

The experimental and calculated spectra for Rh_9^+ are shown in Fig. 4. The experimental spectrum of Rh_9Ar^+ has three intense features at 184, 198, and 236 cm^{-1}. In addition, a weaker band at 271 cm^{-1} and possibly a very weak feature at *ca.* 213 cm^{-1} were also observed.

The lowest energy structure we have found for Rh_9^+ at the PBE1/LANL2DZ level is a trigonal prism capped with three atoms on the square faces (tri) in a 15tet spin multiplicity. The calculated spectrum for this structure has an intense feature at *ca.* 240 cm^{-1} and several weak modes in the range 200–220 cm^{-1} which combine to make a single, broad feature. These match relatively well the strong band at 237 cm^{-1} and the weak feature around 213 cm^{-1} in the experimental spectrum, but do not explain the features at 184, 198, and 271 cm^{-1}. Relatively small changes in the positions and intensities of the calculated modes in the 200–220 cm^{-1} region, (i.e., an increase in intensity and a small red-shift) consistent with the general levels of agreement we observe for other cluster
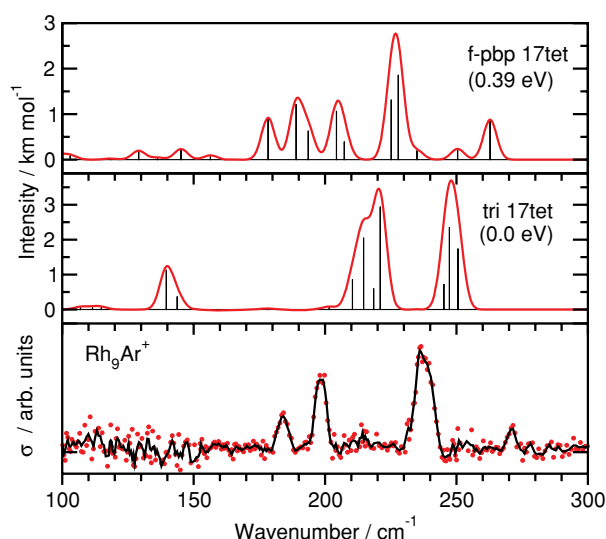
FIG. 5. The spectra of the tri and f-pbp isomers of Rh_9^+ calculated at the TPSSh/def2-TZVP level.

sizes, might explain the features at 184 and 198 cm^{-1} but would still not explain the band at 271 cm^{-1}.

The second-lowest energy geometric structure (15tet f-pbp, 0.35 eV) might provide a match to all of the features in the experimental spectrum. However, the relative intensities of the features are very different, in particular, the band at 213 cm^{-1} is very weak while in the calculation this is the most intense feature.

The spectrum of the 17tet f-pbp isomer calculated at the TPSSh/def2-TZVP level (Fig. 5) is a relatively good match to the features in the experiment, except for the band at 211 cm^{-1} which is calculated to have too high an intensity. However, this is only the third lowest energy isomer (0.39 eV) at this level. The spectra of the two isomers calculated at these two levels appear rather different. Most of the differences appear to come from changes in the relative intensities of the bands, while the changes in positions are smaller and more uniform.

On the basis of this comparison of the spectra we are not able to determine if one or both of these isomers, tri and f-pbp, is present in the experimental population.
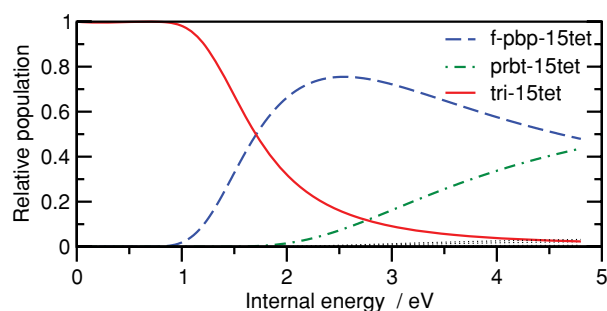

FIG. 6. The population of different isomers of Rh_9^+ as a function of internal energy calculated using the HSA in the microcanonical ensemble based on DFT calculations at the PBE1/LANL2DZ level. The three isomers which are predicted to be significantly populated are shown by the solid, dashed and dash-dot lines and the other isomers by the dotted black lines.

In an effort to investigate the finite temperature properties of the system we have calculated the population distribution of the different isomers as a function of internal energy using the harmonic superposition approximation[43] (HSA) in the microcanonical ensemble. The HSA allows the calculation of ensemble properties from a set of local minima on the PEL and includes effects due to the symmetry and vibrational density of states of the different minima. All of the isomers we have identified for Rh_9^+ at the PBE1/LANL2DZ level were included in the HSA calculation in their lowest energy spin multiplicity. The results, shown in Fig. 6 suggest that the f-pbp isomer may contribute significantly to the population, as it is found to be the first isomer to coexist with the putative global minimum (tri) and it dominates the population over a significant range of internal energies, presumably due to its lower symmetry.[45] The population distribution determined from the HSA calculation is highly sensitive to the relative energies of the different isomers, which is the likely source of the discrepancy in the internal energy at which f-pbp becomes significantly populated (>1 eV) according to the HSA calculation and the internal energy of the clusters in the experiment (∼ 0.2 eV if thermalized at 173 K). This analysis therefore supports the possibility that we may observe one or both of the tri and f-pbp isomers while suggesting that the relative energy differences calculated at the PBE1/LANL2DZ level are too large.

E. Rh_{10}^+

The experimental spectral features of $Rh_{10}Ar_n^+$ species are extremely weak, with very low levels of depletion compared to those of the neighboring $Rh_9Ar_n^+$ and $Rh_{11}Ar_n^+$. As the spectra are measured simultaneously, we are confident that this is a real feature of the spectrum and not due to low cluster signal or poor overlap of the molecular and IR beams. Broad, weak bands are visible in the spectrum of $Rh_{10}Ar_2^+$ at ca. 157 and 245 cm^{-1}, shown in Fig. 7. Our DFT calculations may help to explain these experimental observations, as the four lowest energy geometric structures we have identified lie within 0.02 eV of each other. These are an edge-sharing octahedral (eso) isomer, an icosahedral fragment similar to the Sutton–Chen global minimum (sc1) and two rather amorphous polytetrahedral isomers (o2 and sc3), all of 18tet spin multiplicity. Such small energy separations suggest not only that all of the isomers may be populated, reducing the intensity of any one mode, but also that interconversion between the isomers may occur below the energy necessary to drive the dissociation of the argon atom(s). This would be expected to further decrease the experimental, FIR-MPD, cross section; as a given isomer is excited resonantly by the IR beam it may be heated sufficiently to allow its isomerization, hence depleting the IR absorbing species, but not the intensity of the argon-tagged clusters. The most intense features in the calculated spectra also correspond relatively well to the broad bands in the experimental spectrum.

Beyer and Knickelbein have reported the neutral Rh_{10} cluster to have a fluxional structure on the timescale of their electric deflection experiments.[6] The timescales over which the FIR-MPD and electric deflection experiments are
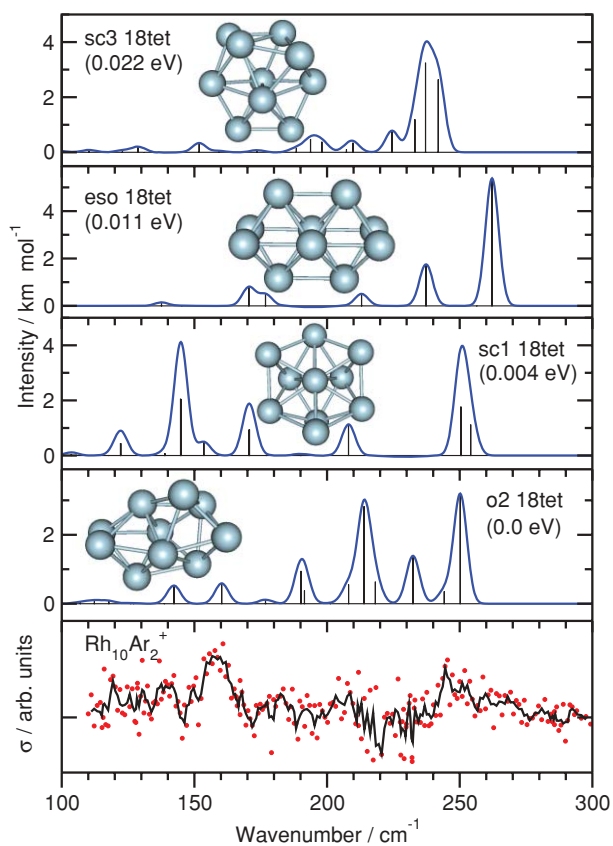
FIG. 7. Experimental spectrum of $Rh_{10}Ar^+$ and calculated spectra of Rh_{10}^+ at the PBE1/LANL2DZ level.

FIG. 8. Experimental spectrum of $Rh_{11}Ar^+$ and calculated spectra of Rh_{11}^+ at the PBE1/LANL2DZ level of theory.

sensitive are somewhat different. Assuming the molecular beam speed is of the order of 1000 ms^{-1}, the time-of-flight through the electric deflection pole (0.31 m long) is some hundreds of microseconds, while the FELIX IR pulse length is typically 5 μs. However, the clusters start colder in the electric deflection experiment (between 49 and 148 K) and are not then heated by IR absorption. Therefore, isomerization would be expected to occur more rapidly in our experiment. While it is not certain that the neutral and cationic cluster PELs are the same,[44,60] this supports our interpretation of the presence of multiple isomers of Rh_{10}^+ and the possibility of isomerization occurring on timescales similar to, or shorter than, that of the experiment.

F. Rh_{11}^+

Figure 8 shows the comparison of the experimental and calculated spectra of Rh_{11}^+. The best agreement between experiment and calculation is observed for a slightly distorted icosahedral fragment (ih-f) isomer in a 17tet spin multiplicity. This corresponds to the lowest energy geometry we have found, but the 17tet is not the optimum spin multiplicity (which is the 19tet in this case). The calculated spectrum matches the experiment quite well in the region above 220 cm^{-1} both in position and intensity. At lower wavenumber the calculated intensities differ significantly from the experiment though the positions of the features still appear to coincide.
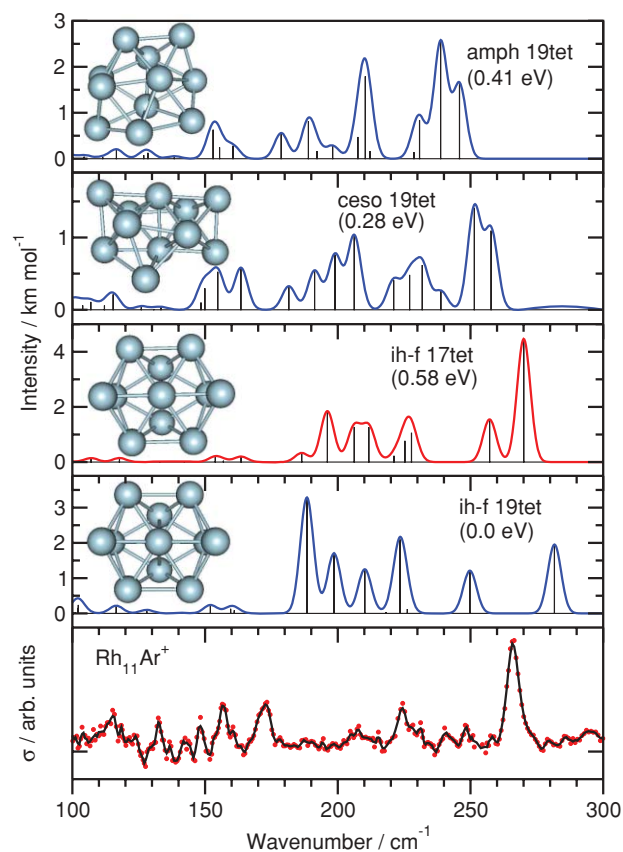
For the other geometric isomers, a capped edge-sharing-octahedral isomer (ceso) and a rather amorphous structure (amph), the agreement is worse. In both cases, the highest calculated frequency is significantly lower than the highest frequency band observed in the experiment.

G. Rh_{12}^+

The experimental spectrum of $Rh_{12}Ar^+$ (see Fig. 9) has a strong feature at 212 cm^{-1}, three weaker features between 250 and 270 cm^{-1} and several weak features below 150 cm^{-1}. The lowest energy structure we have identified (ohc) is based on octahedral units, similar to the bc-oh structure of the Rh_8^+ cluster, but the calculated spectrum is a poor match to the experiment. The second-lowest energy structure (layers), consisting of two roughly planar layers each with six atoms, provides a much better match to the experiment; it matches the strong feature at 212 cm^{-1} to within 2 cm^{-1} and has several features between 250 and 270 cm^{-1}. As for Rh_{11}^+, the agreement is less good at lower wavenumber. In particular, the relatively strong peak calculated to appear at 172 cm^{-1} was not observed in the experiment.

Our proposal here that we have observed an isomer of higher energy is not particularly surprizing as multiple reactive forms of Rh_{12}^+ have been observed with small hydrocarbons[13] and N_2O.[16] It is more surprising that we observe only a single isomer, but this may be due to the very different source conditions (room temperature versus 173 K,
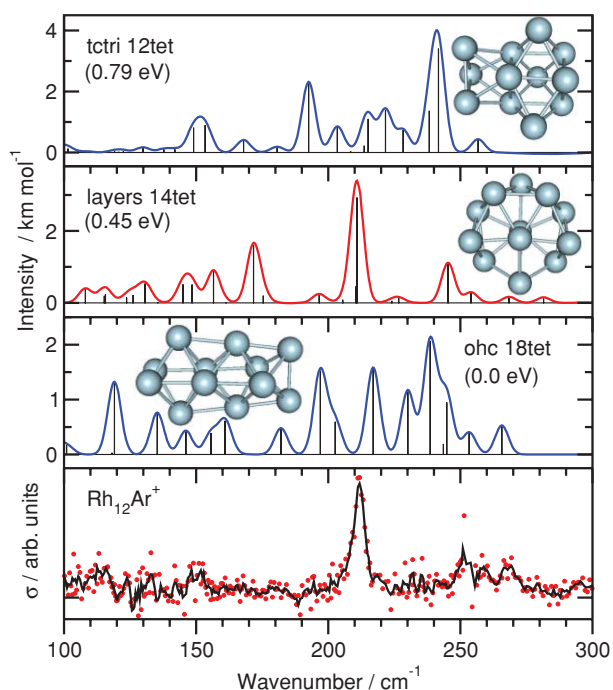
FIG. 9. Experimental spectrum of $Rh_{12}Ar^+$ and calculated spectra of low-energy Rh_{12}^+ isomers at the PBE1/LANL2DZ level of theory.

different He pulse characteristics, and the different time scales of the experiments) though it would be expected that these differences would favor the appearance of the lowest energy structure in the FIR-MPD experiment compared to the FT-ICR reactivity studies. There are several possible causes for this discrepancy, including: (i) the DFT calculations at the PBE1 level may predict an incorrect energy ordering, though to a lesser degree than PBE,[32] (ii) dynamic factors may lead to kinetic trapping of a higher energy isomer,[44] (iii) the lowest energy structure may also be present but have too low a cross section to be observed, or (iv) the global minimum may not bind argon as effectively as this candidate structure.

V. DISCUSSION

As we have previously reported,[32] the favored geometric structure of the Rh_8^+ cluster depends strongly on the inclusion of a fraction of Hartree–Fock exchange. The comparison with experiment suggested that the hybrid PBE1 functional provides a better description of the cluster PEL. Comparison of the FIR-MPD spectra with the results of our calculations using the PBE1 functional across the different cluster sizes presented here further supports our previous finding. Table I shows a comparison of the putative global minimum structures at both PBE and PBE1 levels and the relative energies of these structures calculated using the other functional. It is clear that, at least in some cases, the calculated spectra can be very sensitive to spin multiplicity as well as cluster geometry. In many cases, the best agreement between experimental and calculated spectra was found for the geometry corresponding to the putative global minimum, but not in the lowest energy spin multiplicity.

The fact we get relatively good agreement with the spectra of the low-energy geometries across several sizes gives us some confidence that it is not accidental agreement, and that the PBE1 functional gives a reasonable description of the geometric structure of these rhodium clusters. A reliable description of the spin multiplicity and electronic structure for these highly open-shell systems appears to remain a challenge. This deficiency would not have been apparent for other, low-spin, TM cluster systems,[52,59,60] where very good agreement has previously been obtained between experimental spectra and those derived from pure exchange-correlation functionals but may, in part, explain the difficulties experienced with high-spin cobalt clusters.[63] Further, the relative success of the hybrid functional in describing these high-spin Rh clusters is unexpected, given that hybrid functionals are generally found to provide a relatively poor description of the properties of bulk d-metals compared to pure density dependent functionals.[61] However, most of the properties compared in this study are perhaps not the most relevant when applied to cluster systems, or even surfaces.

The structures we identified in this work are similar to those determined for vanadium,[62] niobium,[60] tantalum,[52] and most cobalt clusters, with the exception of the seven-atom clusters.[63] We find no evidence for cubic motifs in any of the cluster sizes investigated. Though in many cases the structures favored by the pure PBE functional have cubic motifs, the spectra calculated for these isomers are in poor agreement with the experimental spectra (Fig. S1).[57] In general, the close-packed structures favored by the hybrid functional were supported by the pure functional (albeit at higher relative energies), whilst some of the open structures favored by the pure functional were found to be transition states or prone to collapse when reoptimized with the hybrid functional. The structures, relative energies, and spectra calculated with the PBE and TPSSh functionals are available in the ESI. As we have previously noted[32] in the case of the bc-oh isomer of Rh_8^+, the spectra calculated for a given geometry with pure and hybrid functionals can differ significantly, apparently due to small structural differences and the degree of distortion away from an "ideal" high symmetry geometry.

These complications notwithstanding, there does not appear to be any obvious correlation between the structures of the clusters we identify and the trends in reactivity which have been previously observed. One suggestion, in addition to the arguments presented above, is that the electronic structure, in part determined by the geometry, plays a key role in governing the reactivity of small rhodium clusters. The determination of the geometric structures should, however, facilitate further in-depth experimental and theoretical studies of the electronic structures of these clusters.

Another, broader, issue to emerge from our findings concerns the reliability of DFT when applied to high-spin systems such as these Rh clusters. Our results give a very strong indication that hybrid exchange-correlation functionals are superior to pure functionals in describing these systems, at least in terms of the geometry. The performance of these hybrid functionals may not be perfect; however, given the inconsistencies in spin multiplicity that we have noted when comparing experimental and calculated IR spectra. Clearly, more work

TABLE I. Cross-comparison of the putative global minimum (PGM) obtained with one functional with the lowest energy spin-state (found using this functional) of the favored geometric structure (FGS) from the second functional. ‡Structure not investigated at the PBE level. * Structure collapsed during optimization.

Size n	PBE1					PBE				
	PGM_{PBE1}	$2S+1$	FGS_{PBE}	$2S+1$	ΔE / eV	PGM_{PBE}	$2S+1$	FGS_{PBE1}	$2S+1$	ΔE / eV
6	oh	10	oh	10	0.0	oh	10	oh	10	0.0
7	pbp	11	pbp	11	0.0	pbp	11	pbp	11	0.0
8	bc-oh	14	cube	12	0.92	cube	8	bc-oh	14	0.34
9	tri	13	ccube	15	1.14	ccube	11	tri	11	0.11
10	o2	18	eso	18	0.01	eso	16	o2	‡	‡
11	ih-f	19	ceso	19	0.28	ceso	17	ih-f	*	*
12	ohc	18	boxkite	8	1.96	boxkite	8	ohc	16	2.00

is required to determine the factors underpinning the performance of the hybrid functionals in this case. This comparative study provides a fundamental basis from which to begin this endeavor, particularly for Rh_6^+, where the system size may be small enough to consider using current multireference approaches, and where we are now reasonably confident of the structure. These calculations could be used to inform new developments of exchange-correlation functionals with improved structural prediction for TM clusters in particular, and more reliable performance for high-spin systems in general.

VI. CONCLUSIONS

The geometric structures of small cationic rhodium clusters Rh_n^+ ($n = 6$–12) have been investigated by comparison of experimental FIR-MPD spectra and spectra calculated using DFT. Close-packed structures based on octahedral and tetrahedral motifs were found to provide the best matches for most of the clusters considered. The hybrid PBE1 exchange-correlation functional was found to provide a reasonable description of the geometric structures of these clusters. However, challenges still remain in using DFT to gain a reliable description of the electronic structure of these systems, principally the spin multiplicity. The joint experimental and theoretical findings presented here will enable future development of functionals with improved performance for these challenging systems.

[1] M. Knickelbein, Annu. Rev. Phys. Chem. **50**, 79 (1999).

[2] J. A. Alonso, Chem. Rev. **100**, 637 (2000).

[3] P. B. Armentrout, Annu. Rev. Phys. Chem. **52**, 423 (2001).

[4] A. J. Cox, J. G. Louderback, and L. A. Bloomfield, Phys. Rev. Lett. **71**, 923 (1993).

[5] A. J. Cox, J. G. Louderback, S. E. Apsel, and L. A. Bloomfield, Phys. Rev. B **49**, 12295 (1994).

[6] M. K. Beyer and M. B. Knickelbein, J. Chem. Phys. **126**, 104301 (2007).

[7] M. R. Zakin, D. M. Cox, and A. Kaldor, J. Chem. Phys. **89**, 1201 (1988).

[8] C. Berg, M. K. Beyer, T. Schindler, G. Niedner-Schatteburg, and V. E. Bondybey, J. Chem. Phys. **104**, 7940 (1996).

[9] G. Albert, C. Berg, M. K. Beyer, U. Achatz, S. Joos, G. Niedner-Schatteburg, and V. E. Bondybey, Chem. Phys. Lett. **268**, 235 (1997).

[10] C. Berg, M. K. Beyer, U. Achatz, S. Joos, G. Niedner-Schatteburg, and V. E. Bondybey, J. Chem. Phys. **108**, 5398 (1998).

[11] I. Balteanu, O. Balaj, B. Fox-Beyer, P. Rodrigues, M. Barros, A. Moutinho, M. Costa, M. Beyer, and V. Bondybey, Organometallics **23**, 1978 (2004).

[12] M. S. Ford, M. L. Anderson, M. P. Barrow, D. P. Woodruff, T. Drewello, P. J. Derrick, and S. R. Mackenzie, Phys. Chem. Chem. Phys. **7**, 975 (2005).

[13] C. Adlhart and E. Uggerud, J. Chem. Phys. **123**, 214709 (2005).

[14] C. Adlhart and E. Uggerud, Int. J. Mass Spectrom. **249**, 191 (2006).

[15] M. L. Anderson, M. S. Ford, P. J. Derrick, T. Drewello, D. P. Woodruff, and S. R. Mackenzie, J. Phys. Chem. A **110**, 10992 (2006).

[16] D. Harding, M. S. Ford, T. R. Walsh, and S. R. Mackenzie, Phys. Chem. Chem. Phys. **9**, 2130 (2007).

[17] B. Reddy, S. Nayak, S. Khanna, B. Rao, and P. Jena, Phys. Rev. B **59**, 5214 (1999).

[18] L. Wang and Q. Ge, Chem. Phys. Lett. **366**, 368 (2002).

[19] T. Futschek, M. Marsman, and J. Hafner, J. Phys.: Condens. Matter. **17**, 5927 (2005).

[20] V. Bertin, R. Lopez-Rendón, G. del Angel, E. Poulain, R. Avilés, and V. Uc-Rosas, Int. J. Quantum Chem. **110**, 1152 (2010).

[21] Y.-C. Bae, H. Osanai, V. Kumar, and Y. Kawazoe, Phys. Rev. B **70**, 195413 (2004).

[22] Y.-C. Bae, V. Kumar, H. Osanai, and Y. Kawazoe, Phys. Rev. B **72**, 125427 (2005).

[23] F. Aguilera-Granja, L. C. Balbás, and A. Vega, J. Phys. Chem. A **113**, 13483 (2009).

[24] L.-L. Wang and D. D. Johnson, Phys. Rev. B **75**, 235405 (2007).

[25] L.-L. Wang and D. D. Johnson, J. Phys. Chem. B **109**, 23113 (2005).

[26] Y. Sun, R. Fournier, and M. Zhang, Phys. Rev. A **79**, 043202 (2009).

[27] J. P. Chou, H. Y. T. Chen, C. R. Hsing, C. M. Chang, C. Cheng, and C. M. Wei, Phys. Rev. B **80**, 165412 (2009).

[28] D. J. Wales, M. A. Miller, and T. R. Walsh, Nature (London) **394**, 758 (1998).

[29] H. Wang, H. Haouari, R. Craig, Y. Liu, J. R. Lombardi, and D. M. Lindsay, J. Chem. Phys. **106**, 2101 (1997).

[30] J. D. Langenberg and M. D. Morse, J. Chem. Phys. **108**, 2331 (1998).

[31] R. V. Zee, Y. Hamrick, S. Li, and W. Weltner, Jr., Chem. Phys. Lett. **195**, 214 (1992).

[32] D. J. Harding, T. R. Walsh, S. M. Hamilton, W. S. Hopkins, S. R. Mackenzie, P. Gruene, M. Haertelt, G. Meijer, and A. Fielicke, J. Chem. Phys. **132**, 011101 (2010).

[33] D. J. Wales and J. P. K. Doye, J. Phys. Chem. A **101**, 5111 (1997).

[34] A. P. Sutton and J. Chen, Philos. Mag. Lett. **61**, 139 (1990).

[35] D. Harding, S. R. Mackenzie, and T. R. Walsh, J. Phys. Chem. B **110**, 18272 (2006).

[36] M. J. Frisch, G. W. Trucks, H. B. Schlegel, G. E. Scuseria, M. A. Robb, J. R. Cheeseman, J. A. Montgomery, Jr., T. Vreven, K. N. Kudin, J. C. Burant, *et al.* Gaussian, Inc., Pittsburgh PA (2003).

[37] J. C. Slater, Phys. Rev. **81**, 385 (1951).

[38] S. H. Vosko, L. Wilk, and M. Nusair, Can. J. Phys. **58**, 1200 (1980).

[39] J. P. Perdew, K. Burke, and M. Ernzerhof, Phys. Rev. Lett. **77**, 3865 (1996).

[40] J. P. Perdew, M. Ernzerhof, and K. Burke, J. Chem. Phys. **105**, 9982 (1996).

[41] P. Fuentelba, H. Preuss, H. Stoll, and L. v. Szentpalt, Chem. Phys. Lett. **89**, (1989).

[42] P. J. Hay and W. R. Wadt, J. Chem. Phys. **82**, 270 (1985).

[43] D. J. Wales, Mol. Phys. **78**, 151 (1993).

[44] T. R. Walsh, J. Chem. Phys. **124**, 204317 (2006).

[45] D. J. Harding, R. D. L. Davies, S. R. Mackenzie, and T. R. Walsh, J. Chem. Phys. **129**, 124304 (2008).

[46] J. Tao, J. P. Perdew, V. N. Staroverov, and G. E. Scuseria, Phys. Rev. Lett. **91**, 146401 (2003).

[47] V. N. Staroverov, G. E. Scuseria, J. Tao, and J. P. Perdew, J. Chem. Phys. **119**, 12129 (2003).

[48] F. Weigend and R. Ahlrichs, Phys. Chem. Chem. Phys. **7**, 3297 (2005).

[49] R. Ahlrichs, M. Bär, M. Häser, H. Horn, and C. Kölmel, Chem. Phys. Lett. **162**, 165 (1989).

[50] O. Treutler and R. Ahlrichs, J. Chem. Phys. **102**, 346 (1995).

[51] M. P. Johansson, A. Lechtken, D. Schooss, M. M. Kappes, and F. Furche, Phys. Rev. A **77**, 053202 (2008).

[52] A. Fielicke, P. Gruene, M. Haertelt, D. J. Harding, and G. Meijer, J. Phys. Chem. A **114**, 9755 (2010).

[53] A. Fielicke, G. Meijer, and G. von Helden, Eur. Phys. J. D **24**, 69 (2003).

[54] A. Fielicke, A. Kirilyuk, C. Ratsch, J. Behler, M. Scheffler, G. von Helden, and G. Meijer, Phys. Rev. Lett. **93**, 023401 (2004).

[55] D. Oepts, A. F. G. van der Meer, and P. W. van Amersfoort, Infrared Phys. Technol. **36**, 297 (1995).

[56] M. Reiher, O. Salomon, and B. A. Hess, Theor. Chim. Acta **107**, 48 (2001).

[57] See supplementary material at http://dx.doi.org/10.1063/1.3509778 for details of the quantum chemical calculations.

[58] S. Gilb, P. Weis, F. Furche, R. Ahlrichs, and M. M. Kappes, J. Chem. Phys. **116**, 4094 (2002).

[59] P. Gruene, D. M. Rayner, B. Redlich, A. F. G. van der Meer, J. T. Lyon, G. Meijer, and A. Fielicke, Science **321**, 674 (2008).

[60] A. Fielicke, C. Ratsch, G. von Helden, and G. Meijer, J. Chem. Phys. **127**, 234306 (2007).

[61] J. Paier, M. Marsman, K. Hummer, G. Kresse, I. C. Gerber, and J. G. Ángyán, J. Chem. Phys. **125**, 249901 (2006).

[62] C. Ratsch, A. Fielicke, A. Kirilyuk, J. Behler, G. von Helden, G. Meijer, and M. Scheffler, J. Chem. Phys. **122**, 124302 (2005).

[63] R. Gehrke, P. Gruene, A. Fielicke, G. Meijer, and K. Reuter, J. Chem. Phys. **130**, 034306 (2009).